Magnetic properties of the neptunium monopnictides*

A. T. Aldred, B. D. Dunlap, A. R. Harvey, D. J. Lam, G. H. Lander, and M. H. Mueller

Argonne National Laboratory, Argonne, Illinois 60439
(Received 21 November 1973)

The magnetic properties of the neptunium monopnictides, NpN, NpP, NpAs, and NpSb, have been examined by a variety of experimental techniques. All compounds have the NaCl structure. The present paper reports the results of magnetization, Mössbauer, electrical-resistivity, neutron-diffraction, and lattice-parameter (x-ray) measurements between 1.5 and 300 °K on polycrystalline samples prepared in this laboratory. Particular emphasis is placed on both the complementary information obtained by the different techniques, and how this helps to elucidate the microscopic magnetic behavior. Neptunium nitride is ferromagnetic with $T_C = 87$ °K. Neptunium phosphide orders antiferromagnetically at 130 °K with an incommensurate magnetic structure. At 74 °K the magnetic structure becomes commensurate with the lattice (repeat distance 3.0 unit cells) and at lower temperatures tends to form a 3+, 3− sequence. A complete solution for the magnetic structure at low temperature is obtained by combining the neutron and Mössbauer results. Neptunium arsenide becomes antiferromagnetic at $T_N = 175$ °K. At ~ 160 °K, the high-temperature 4+, 4− structure transforms to the type-I arrangement (simple +, − sequence). The crystal lattice of NpAs becomes tetragonal at T_N, exhibits a first-order transition to cubic symmetry at 142 °K, and remains cubic at lower temperatures. The electrical resistivity increases by an order of magnitude on cooling from 142 to 141 °K. Neptunium antimonide is a type-I antiferromagnet with $T_N = 207$ °K. The variation of the ordered moments (1.4μ_B/Np in NpN to 2.5μ_B/Np in NpSb), paramagnetic effective moment ($\sim 2.5\mu_B$/Np), and the Mössbauer parameters (hyperfine field, quadrupole interaction, and isomer shift) all suggest a trend toward Np^{3+}, $5f^4$ free-ion behavior in progressing from the nitride to the antimonide.

I. INTRODUCTION

The magnetic properties of the uranium monopnictides (Uv, where v is an element of group V) and monochalcogenides (Uvi, where vi is an element of group VI) have been examined in detail over the last decade.[1] The early actinide metals are nonmagnetic,[2] and attempts to understand both the origins of magnetism and the nature of the magnetic ordering in actinide compounds have naturally started with those compounds that are the most available and have the simplest crystal structure. The Uv and Uvi series, as well as the analogous neptunium compounds, all have the NaCl crystal structure. Perhaps the most interesting feature of the magnetic properties of the Uv compounds is the multiple transitions that occur in UP and UAs. Recently, these transitions have also been the subject of theoretical studies.[3,4] In an effort to learn more about these low-temperature transitions and about the exchange processes in the Uv compounds in general, a number of experiments have been performed on the solid solutions between Uv and Uvi, for example, UP-US,[5] UAs-US,[6] UAs-USe.[7]

Considerable strides have been made recently in understanding the magnetic behavior of the lanthanide monopnictides and monochalcogenides in terms of the interaction between the electrostatic crystal-field and interatomic exchange interactions.[8] The same interactions presumably play a role in 5f-electron systems, but analyses similar to those used in the lanthanide series have not been quanti-

tatively successful. The large variety of magnetic behavior observed in the early actinide metals and in their compounds is strongly related to the interatomic distances between the actinide ions in the solid and the subsequent degree of localization of the 5f electrons. The greater overlap of neighboring 5f orbitals favors larger bandwidths which, when larger than the Coulomb correlation energy, lead to itinerant-electron magnetism. The bandwidth is effectively increased by the hybridization of the 5f and 6d-7s-7p bands. If the overlap of neighboring 5f orbitals is relatively small, the 5f electrons are essentially localized and this often results in magnetic ordering. In addition, the greater spatial extent of the 5f-electron wave functions, as compared with those of the 4f series, leads to stronger interactions between the 5f electrons and both the conduction band and crystalline environment.

The study of the Npv compounds represents an important advance in our attempt to characterize and understand actinide magnetism. We report here magnetic-susceptibility, Mössbauer, electrical-resistivity, neutron, and low-temperature x-ray-diffraction experiments. A number of these results have been reported earlier, usually at conferences, by various permutations of the present authors. In the present paper we consolidate this information and present new results. One important advantage, apart from the ease of reference, in discussing the results within one publication is that the correlations between the results obtained

with various experimental techniques may be dem-
onstrated clearly.

II. EXPERIMENTAL DETAILS

A. Sample preparation

Neptunium, element 93, does not occur naturally
and the 237 isotope, which has been used through-
out this study, is produced by the $(n, 2n)$ reaction
on ^{238}U in nuclear reactors. This is the most sta-
ble of the neptunium isotopes with a half-life of
2.2×10^6 yr. The isotope is radioactive (primarily
α and γ radiation) and highly toxic. Considerable
care must, of course, be taken at all times in han-
dling neptunium and its compounds. All steps in
the preparation of samples must therefore be per-
formed in glovebox facilities, which contain pure
argon so that the samples are not exposed to an
oxygen atmosphere. For individual experiments
the materials are encapsulated in special sample
holders, which can be removed from the glovebox.

Chemical analysis of the neptunium metal used
in preparing the compounds indicated the presence
of the following impurities in parts per million:
Al, 26; B, 2; Ca, 30; Cr, 19; Cu, 10; Fe, 94;
Mg, 60; Mn, 3; Mo, 2; Ni, 29; Pb, 5; Si, 178;
Ti, 5; N, 11; O, 312; H, 7; and C, 73. The total
impurity content of the high-purity gases used to
prepare the compounds was less than 1 ppm. The
final compounds were not chemically analyzed, but
in previous experiments the oxygen content in com-
pounds identically prepared was ~ 0.2% with less
than 100 ppm of nitrogen or carbon.

The compounds NpN, NpP, and NpAs were pre-
pared by reacting NpH_3 with nitrogen, phosphine,
and arsine gas, respectively, at temperatures in
the range 300–350 °C for 5 h. The powdered sam-
ples were pressed into pellets and homogenized at
1000 °C for $2\frac{1}{2}$ h. The NpSb was prepared by an iso-
thermal annealing technique.[9] In this technique,
equal atomic percentages of neptunium and
99.999%-pure antimony are sealed in a quartz tube
under vacuum, and the mixture is heated at the
melting temperature of antimony. The tempera-
ture is then raised to 1000 °C, held at this temper-
ature for 16 days, and then cooled. X-ray-dif-
fraction patterns were used to identify the struc-
ture (NaCl in all cases) and to measure the lattice
parameter. In all samples of NpSb, traces of
Np_3Sb_4 were present; attempts to make NpBi were
unsuccessful. No additional phases were observed
in the samples of NpN, NpP, and NpAs.

B. Experimental techniques

Magnetization measurements were made using a
conventional force technique[10] in magnetic fields be-
tween 1 and 10.7 kOe and in the temperature range
of 1.5–300 °K. The susceptibilities were obtained

by taking data at six (or more) fields up to 10.7
kOe, fitting the results to a two-term equation (lin-
ear in $1/H$), and extrapolating to $1/H = 0$. Hyper-
fine spectra were obtained between 4.2 and 78 °K
using the 59.6-keV Mössbauer resonance of ^{237}Np
with a source of ^{241}Am in α-Am metal.[11]

Neutron-diffraction patterns were obtained with a
two-axis diffractometer at the CP-5 Research Re-
actor.[6] The polycrystalline samples, between 1.8
and 3.2 g, were contained in thin-wall vanadium
capsules (0.63-cm diam) i· ⌐ variable-temperature
(2.2–300 °K) cryosta⁺ ⌐ne neutron patterns pro-
vide a direct test of ⌐ne sample stoichiometry,
since the intensities of the diffraction lines with
hkl even are proportional to $(b_{Np} + b_{anion})$, where b
represents a nuclear scattering length, and those
reflections with hkl odd are proportional to the dif-
ference $(b_{Np} - b_{anion})$. In all cases, the intensities
of the room-temperature pattern were in excellent
agreement with those expected from considerations
of the nuclear scattering lengths.[12] We estimate
that the 1 : 1 stoichiometry is correct to within 2%
for all compounds. The magnetic form factor used
in interpreting the present neutron intensities is
that determined in studies of uranium compounds.[5,6]
For low scattering angles $(\sin\theta/\lambda \leq 0.3 \text{ Å}^{-1})$, the
dipole approximation[13] is certainly sufficient, and
all actinide form factors will be essentially the
same. The low-temperature x-ray experiments
were performed on the samples used in the neutron
investigations. The powder was die pressed (527
kg/cm²) into a flat disk and placed in a milled re-
cess in a copper sample holder. The disk was
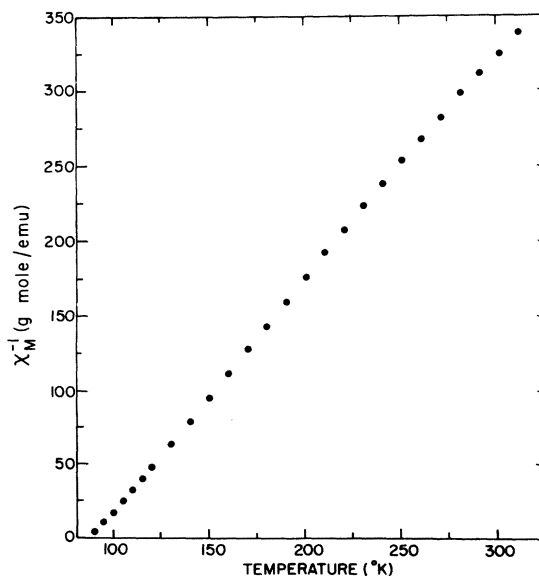covered with a Mylar window (0.005 cm thick) and

FIG. 1. Inverse susceptibility as a function of tempera-
ture for NpN.

sealed with a small copper frame and epoxy resin. The sample holder was attached with vacuum grease to a large copper block in a variable-temperature cryostat. Measurements were made on a conventional diffractometer table with filtered Cu $K\alpha$ radiation.

Electrical-resistivity measurements were made between 1.5 and 300 °K using a standard direct-current four-probe technique.[14] The samples were shaped from pieces of the flat disks employed in the x-ray experiments and had nominal dimensions of 1×1×7 mm. The disks were fragile, and it was difficult to obtain samples with a uniform cross section. In addition, the material was somewhat porous. Although density measurements were not performed on the material, it is estimated that the disks had 80–90% of the theoretical density. As a result of these factors, the absolute values of the resistivities reported here may be seriously in error. Our main interest, however, is in the temperature dependence of the resistivity.

III. RESULTS

A. NpN

De Novion and Lorenzelli[15] reported that NpN is ferromagnetic, with a Curie temperature of 82 °K. Previous magnetization measurements by one of us[16] suggested a Curie temperature of 100 ± 2 °K. The results of other experiments reported here (neutron diffraction, x-ray diffraction, and resistivity) give a transition temperature in the range
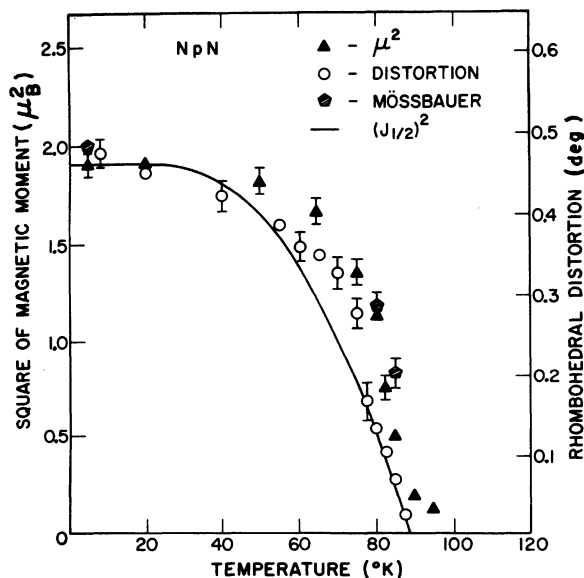

FIG. 2. Temperature dependence of the square of the magnetic moment (neutron diffraction), rhombohedral distortion (x rays), and the square of the neptunium hyperfine field (Mössbauer) in NpN. The solid curve is the $(J_{1/2})^2$ function.

84–89 °K. The spread in values is probably related to the existence of magnetic short-range order that is observed up to 105 °K in the neutron-diffraction measurements.

We have undertaken a new series of magnetization measurements on NpN. Our low-temperature data (below 70 °K) are in good agreement with the results given in Fig. 1 of Ref. 16. The substantial field dependence of the magnetization indicates a large magnetocrystalline anisotropy typical of actinide ferromagnets, e.g., US.[17,18] The magnetization at the highest field corresponds to a moment of ~0.9μ_B/(Np atom). Conventional extrapolation techniques (e.g., versus H^{-1} or H^{-2}) yield poor fits to the data, and the saturation moment cannot be determined reliably. However, a magnetic moment of $(1.38 \pm 0.07)\mu_B$/(Np atom) is obtained from the neutron-diffraction experiments, and the hyperfine field determined by the Mössbauer technique is in good agreement with this value. (The relationship between the Mössbauer hyperfine field and the magnetic moment as determined by neutron diffraction is essentially linear in the Npv compounds, see Sec. IV and Fig. 15.) Between 140 and 310 °K, the magnetization σ is linear in field H, and the susceptibility was determined as σ/H. Below 140 °K, curvature becomes evident in the σ-vs-H plots, and the susceptibility was determined by linear extrapolation of σ^2-vs-H/σ plots to $H=0$. Measurements were made at 1 °K intervals below 100 °K, and the data indicate that the sample was paramagnetic at 87 °K and ferromagnetic at 86 °K. This result is now consistent with the values given by the other measurements, and we would suggest a Curie temperature of 87 ± 3 °K for NpN. The quoted uncertainty indicates that the bulk magnetic transition probably does not occur in our sample at a single temperature. A plot of the reciprocal molar susceptibility as a function of temperature is shown in Fig. 1.

The temperature dependence of the magnetic moment in the ordered state, as determined by neutron diffraction, is plotted in Fig. 2. Since ferromagnetism is revealed in the neutron pattern as additional intensity on the nuclear peaks, the accurate measurement of this additional intensity is often difficult. However, in the case of NpN, the difference peaks. e.g., (111) and (311), in the nuclear pattern are proportional to $b_{Np} - b_N = 1.055 - 0.96 = 0.095 \times 10^{-12}$ cm and are weak. The additional ferromagnetic intensity is thus easily measured; the (111) peak increases by a factor of 6 on cooling the sample from 100 to 5 °K. Also illustrated in Fig. 2 is the temperature dependence of the rhombohedral distortion of the unit cell that is observed by x-ray diffraction in NpN below T_C. In the paramagnetic (cubic) phase, a rhombohedral unit cell with an angle α of 60° may be used to describe the structure. The trigonal axis of this unit

TABLE I. Properties of the Npv compounds. a_0 is the lattice parameter at 300 °K, α is the coefficient of thermal expansion between 150 and 300 °K, $\mu_{\rm eff}$ is the effective paramagnetic moment, θ_p is the paramagnetic Curie temperature, ρ is the electrical resistivity at 300 °K, $1/\tau$ is the repeat distance of the magnetic structure, $\mu_{\rm sat}$ is the ordered moment at 5 °K, $H_{\rm hf}$ is the hyperfine field at the Np nucleus at 5 °K, and e^2qQ is the quadrupole interaction at 5 °K. The isomer shift is relative to $NpAl_2$. The quantity $(c-a)/a$ is a measure of the crystallographic distortion from cubic symmetry in the ordered state.

Parameters	NpN	NpP	NpAs	NpSb
a_0 [Å($\pm$0.001)]	4.897	5.615	5.838	6.254
α [10^{-6}/°K($\pm$1.0)]	5.5	9.6	10.3	17.0
$\mu_{\rm eff}$ [μ_B/F.U. ($\pm$0.15)]	2.4	2.8	2.6	$\sim$2.3
θ_p [°K($\pm$10)]	100	125	$\sim$190	$\sim$150
ρ [$\mu\Omega$ cm($\pm$30%)]	3100	3700	5100	
T_C [°K($\pm$3)]	87			
T_N [°K($\pm$3)]		130	175	207
Magnetic structure	ferro	LW	LW	type I
$1/\tau$ [unit cells ($\pm$0.10)]		2.78	4.00	1.0
Second transition (°K)		74	140–150	
$1/\tau$ (unit cells)		3.00	1.00	
$\mu_{\rm sat}$ [μ_B($\pm$0.1)]	1.4	$\begin{cases}2.3\\1.8\end{cases}$	2.5	2.5
$H_{\rm hf}$ [kOe($\pm$40)]	2730	$\begin{cases}4210\\3690\end{cases}$	4800	4770
e^2qQ [10^{-7} eV($\pm$2)]	+9	$\begin{cases}-28\\-24\end{cases}$	-70	-60
Isomer shift [mm/sec($\pm$1)]	-6	$\begin{cases}+7\\+7\end{cases}$	+16	+20
$(c-a)/a$ [10^{-4}($\pm$3)]	-52 at 5 °K	-42 at 5 °K	-8 at 143 °K $\leq$3 at 5 °K	<15 at 5 °K

cell is the [111] axis of the cubic cell. When the distortion occurs, the [111] axis is either compressed or stretched, and the rhombohedral angle becomes greater than or less than 60°, respectively. A convenient description of this distortion is to define a length c as a distance along the unique trigonal axis and a as a distance in the plane perpendicular to c such that $c/a=1.00$ in the cubic phase. This definition is especially useful in comparing the magnitude of trigonal and tetragonal distortions (see Table I). The relationship between the change in the rhombohedral angle $\Delta\alpha$ and the c/a ratio is then $\Delta\alpha = -(8/\sqrt{27})(c-a)/a$ rad. From symmetry considerations, the rhombohedral distortion in NpN indicates that the magnetic moments lie in, or perpendicular to, the (111) plane. This information cannot be obtained with neutron experiments on polycrystalline ferromagnets. Magnetization[17] and neutron[18] experiments on single crystals of US, which also has a rhombohedral distortion, indicate that the magnetic moments are parallel to the unique trigonal axis.

Included in Fig. 2 is the $(J_{1/2})^2$ Brillouin function, which has the slowest decrease in magnetic moment with temperature within the framework of a simple molecular-field theory. The temperature depen-

dence of the square of the magnetic moment is different from that of the crystallographic distortion, and both are more abrupt than the $J_{1/2}$ Brillouin function. This suggests that higher-order effects modify the spontaneous magnetization process. Marples[19] has reported rhombohedral distortions in US and USe, but of the opposite sign; i.e., the [111] axis stretches in US and USe but is compressed in NpN. Marples used an angle of 90° to characterize the rhombohedral cell in the cubic phase. The relationship between the 60° and 90° cells is such that $\Delta\alpha_{60°} = (4/\sqrt{3})\Delta\alpha_{90°}$. In the case of US, the temperature dependence of the distortion and the magnetization appear to agree, but, recalling the magnetic anisotropy of US,[17] this comparison should be made with neutron or hyperfine-field data. If we consider the neutron results in Fig. 2 to represent $\langle M^2\rangle$ as a function of temperature, then the lattice distortion approximately follows $\langle M^4\rangle$.

The results of the Mössbauer experiments on NpN at 5 °K are given in Table I. Although the spectra are less resolved as T_C is approached, experiments at two higher temperatures were performed. The temperature dependence of the magnetization as determined from the hyperfine field
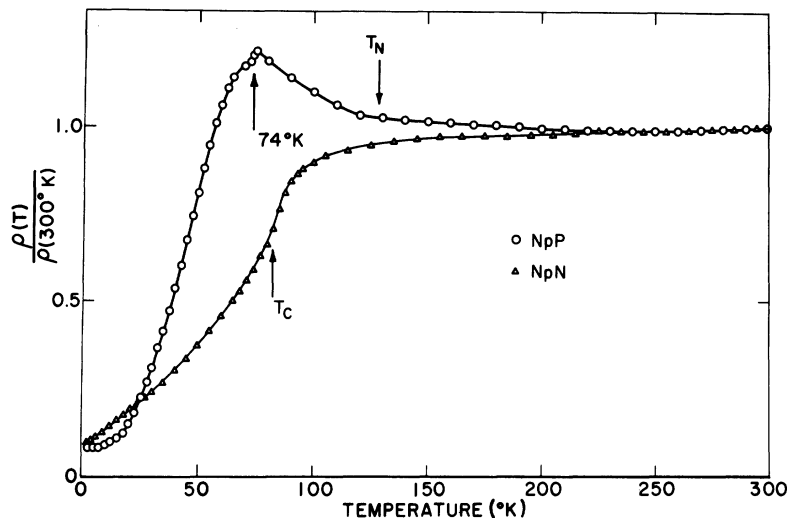
FIG. 3. Electrical resistivities of NpN and NpP (normalized to their values at 300 °K) as a function of temperature.

is shown in Fig. 2 and is in agreement with that determined by neutron diffraction.

The electrical resistivity of NpN (normalized to its value of 300 °K) is shown in Fig. 3. At 300 °K the resistivity (~ 3100 $\mu\Omega$ cm) is considerably higher than that reported by de Novion and Loren-zelli[15] (~ 400 $\mu\Omega$ cm). Experimental uncertainties and differences in the form of the sample probably account for the discrepancy between the absolute values. The temperature dependence as given in Fig. 3 is very similar to that in Ref. 15. The fer-romagnetic ordering in NpN produces a shoulder in the resistivity curve at ~ 85 °K. A value for T_C was obtained from the data by analyzing the deriva-tive of the resistivity with respect to temperature. This derivative exhibits a maximum at $T_C = 84.5 \pm 2.0$ °K.

B. NpP

Reports of the magnetic properties,[20] magnetic structure,[21] lattice parameters at low tempera-ture,[22] and nuclear-magnetic-resonance properties in the paramagnetic state[23] of NpP have been pub-lished. In the present paper many of the details will be omitted, but the main features of this in-teresting magnetic material will be highlighted.

Neutron-diffraction experiments on NpP indicate that it becomes antiferromagnetic at $T_N \simeq 130$ °K. The initial ordering is of the longitudinal-wave type,[6] in which the moments are arranged in ferro-magnetic (001) sheets with the spin direction per-pendicular to the sheets, i.e., $\vec{\mu} \| [001]$, and paral-lel to the propagation direction of the modulation. Between 130 and 74 °K the repeat distance is 2.78 ± 0.08 unit cells, and the modulation of the moment from sheet to sheet is sinusoidal. With this type of ordering, two satellites, indexed as $hkl^{\pm\tau}$, are observed around each reciprocal-lattice point in

the neutron pattern. The wave vector τ of the mag-netic structure is parallel to the c axis and is mea-sured in units of $1/c = c^*$. The repeat distance in real space is given by $1/\tau$, the quantity given in Table I. Type-I antiferromagnetic ordering (as found in the uranium monopnictides) is a special case of the longitudinal-wave (LW) modulation with $1/\tau = 1.0$. In NpP at ~ 70 °K, additional satellites (indexed as $hkl^{\pm 3\tau}$) were observed, and the repeat distance $1/\tau$ changes from 2.78 to 3.00; i.e., the magnetic structure becomes commensurate with the lattice. The amplitudes of the first and third har-monics, derived from the intensities of the first
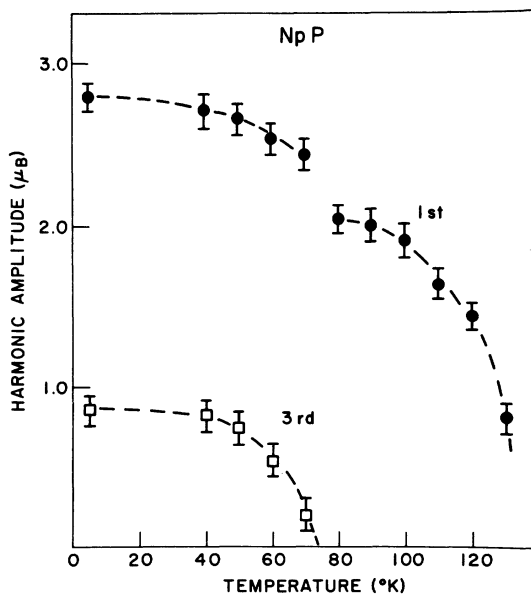

FIG. 4. Temperature dependence of the first and third harmonics for NpP.

and third satellites in the neutron pattern, respectively, are shown in Fig. 4 as a function of temperature. No change in the repeat distance is observed between 70 and 5 °K.

The extensive information obtained from the neutron-diffraction experiments might appear sufficient to determine the precise arrangement of magnetic moments in NpP. This is not, however, the case. Although the amplitudes of the first and third harmonics are known (Fig. 4), the phase angle between these two components of the Fourier series that represent the magnetic arrangement *cannot* be found from neutron measurements. The necessary information is provided by the Mössbauer experiments at 5 °K. The hyperfine spectrum of NpP at 5 °K shows a complex structure that can be analyzed as two overlapping hyperfine patterns having relative intensities 2 : 1. The data and the fitted spectrum are shown in Fig. 5. In the upper portion of the figure, the bar diagram shows the spectrum decomposed into two hyperfine patterns indicated by heavy and light lines. The magnetic hyperfine field (H_{hf}), electric-quadrupole hyperfine coupling (e^2qQ), and isomer shift for the two sites are given in Table I. The Mössbauer spectrum at 5 °K shows that two neptunium moments, one of $\sim 1.9\mu_B$ and the other of $\sim 2.2\mu_B$, are present in the magnetic arrangement, and that atoms with the smaller magnetic moment are twice as numerous as those with the larger. Armed with this important information, we may return to the neutron results and construct a unique model for the magnetic ordering in NpP. The models for the structure at various tempera-
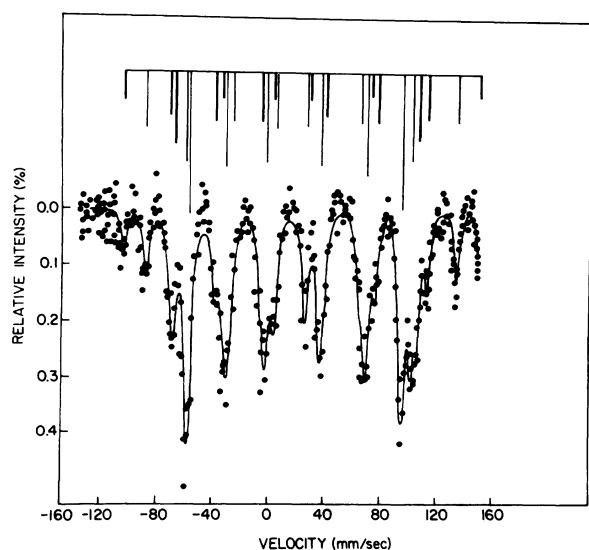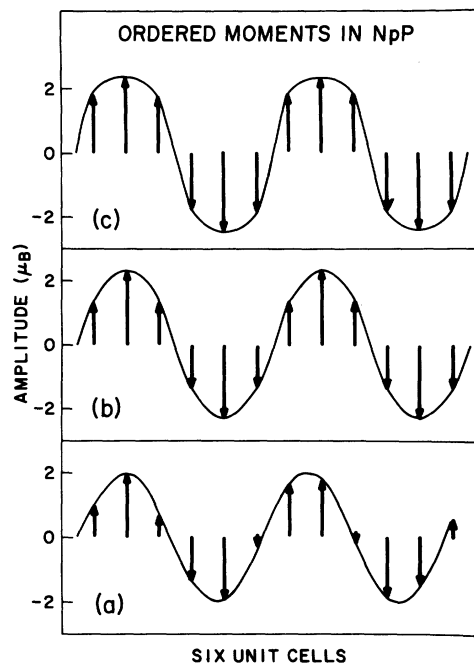

FIG. 6. Models for the localized moments on neptunium atoms in NpP. For convenience, the structure is drawn as a transverse modulation rather than the observed longitudinal-wave modulation. (a) Simple sinusoidal arrangement, existing between 130 and 75 °K. (b) Commensurate structure as at 70 °K. Two complete repeat units are shown. (c) Almost squared-up structure that is present at 5 °K.

tures are shown in Fig. 6. An interesting feature of the magnetic structure at 5 °K [Fig. 6(c)] is that chemically equivalent neptunium atoms have different magnetic moments. Quantitative details of the magnetic-structure determination are given in Ref. 21. The point we wish to emphasize is that neither the neutron nor the Mössbauer experiments can individually unravel the microscopic magnetic properties of NpP, but, taken together, the results from these two techniques give the complete picture in a
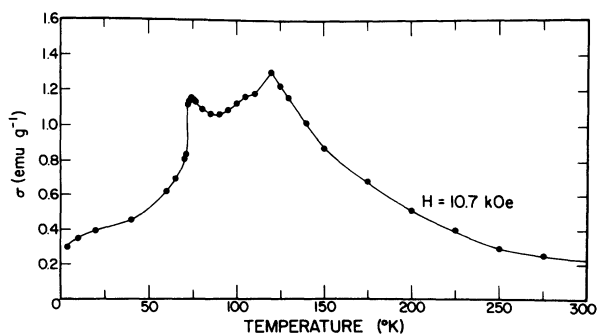

FIG. 5. Hyperfine spectra for ^{237}Np in NpP. The bar diagram at the top shows the decomposition into two separate spectra. The solid line is a least-squares fit yielding the parameters of Table I.

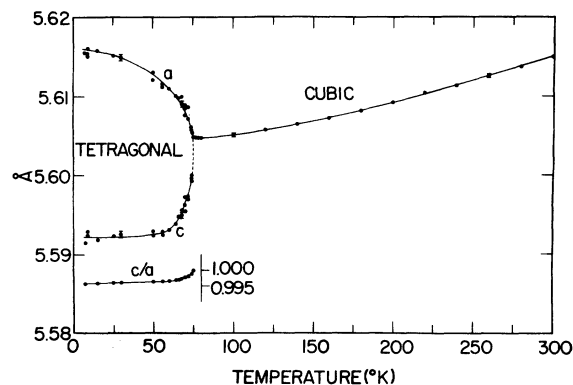FIG. 7. Magnetization of NpP as a function of temperature.

FIG. 8. Variation of the lattice parameter of NpP with temperature. The variation of the c/a ratio in the tetragonal region is also shown.

particularly satisfying manner.

The magnetization of NpP at a field of 10.7 kOe is shown in Fig. 7. The measured susceptibility is independent of the applied field over the entire temperature range. The effective moment in the paramagnetic region (i.e., between 150 and 300 °K) is $(2.8 \pm 0.1)\mu_B/$F.U. (formula unit). The magnetization curve in Fig. 7 shows two anomalies, the first at the Néel temperature of ~130 °K, and the second at 74 ± 1 °K associated with the incommensurate-to-commensurate transition. The sudden drop in magnetization at 74 °K (see Fig. 7) may be understood by noting that the disordered components (i.e., those perpendicular to the propagation direction) of the magnetic structure are substantially reduced in magnitude when the structure becomes commensurate. Compare, for example, the average ordered components as illustrated in Figs. 6(a) and 6(b).

The electrical resistivity of NpP (normalized to its value at 300 °K) is shown in Fig. 3. The room-temperature value of ~3700 $\mu\Omega$ cm is large in comparison with that of both UP (300 $\mu\Omega$ cm) and PuP (750 $\mu\Omega$ cm) and, again, may be in error because of the form of the sample. The Néel temperature is rather poorly defined in the resistivity measurements, except for a change in slope. At 74 °K, however, a sharp drop occurs in the resistivity. This is compatible with a decrease in magnetic scattering when the ordering becomes commensurate with the lattice.

The variation with temperature of the lattice parameter of NpP, as measured by x-ray diffraction, is shown in Fig. 8. No anomaly in the lattice constant is observed at the Néel temperature, but at 74.5 ± 0.3 °K a large tetragonal distortion is observed. The c/a ratio (see insert of Fig. 8) changes abruptly to 0.9975 on cooling 5 °K below the transition, and reaches a value of 0.9958 ± 0.0002 at helium temperature. The volume of the

unit cell ($=a^2c$) shows a discontinuity at 74 °K and expands below this temperature. The volume discontinuity at the incommensurate-commensurate transition implies that this transition is first order. The tetragonal distortion in NpP is, of course, compatible with the tetragonal symmetry of the magnetic structure.[24]

C. NpAs

The compound NpAs becomes antiferromagnetic at $T_N = 175$ °K. The magnetic scattering in the neutron-diffraction pattern between 170 and 160 °K consists of two satellites $hkl^{\pm\tau}$ around each nuclear reflection. As is the case with NpP, the absence of any magnetic scattering at the $(000)^{\pm}$ and $(002)^{\pm}$ positions indicates that the spin direction is parallel to the c axis of the tetragonal magnetic cell, i.e., $\vec{\mu}\|[001]$. The repeat distance $1/\tau = 4.00 \pm 0.15$ unit cells. Thus, unlike the high-temperature phase of NpP, the longitudinal-wave modulation in NpAs is commensurate with the lattice at T_N. The observation of only one order of satellites suggests that the spin modulation is sinusoidal. Unfortunately, in this case, the neutron experiments are not conclusive because the additional intensity expected from a square-wave 4+, 4− modulation would be quite small (see Table II), and, considering the magnitude of the ordered moment (~$1\mu_B$) developed by 160 °K, below our sensitivity. On cooling below 160 °K, further complications occur in the neutron patterns. The intensity of the $(111)^{-1}$ satellite remains constant, but a strong peak is observed to grow with decreasing temperature at the position corresponding to $(111)^{-3}$ and $(111)^{-4}$. These two satellite positions are $2\theta = 15.0°$ and $2\theta = 14.8°$, respectively, and cannot be separated with the angular resolution of the diffractometer. Below 150 °K the intensity of the $(111)^{-4}$, which is equivalent to the (110) reflection with $\tau = 0.25c^*$, increases rapidly. This, together with the presence of other diffraction peaks [for example, the (201) reflection], in-

TABLE II. Intensities of neutron-diffraction peaks [normalized to the type-I (110) magnetic reflection] for various square-wave modulations in NpAs. Neutron wavelength is 1.061 Å, calculations for $\tau = 0.25c^*$ $(1/\tau = 4)$.

Model number	Arrangement	Calculated intensity			
		$(111)^{-\tau}$	$(111)^{-2\tau}$	$(111)^{-3\tau}$	(110) $(111)^{-4\tau}$
1	+ − + − + − + −	0	0	0	100
2	+ + − + − − + −	8	0	80	0
3	+ + − − + − + −	4	20	40	25
4	+ + − − + + − −	0	78	0	0
5	+ + + − − + − −	14	40	24	0
6	+ + + − − − + −	24	20	6	25
7	+ + + + − − − −	50	0	14	0

dicates that the magnetic structure below 140 °K is the familiar type-I ordering, in which ferromagnetic (001) sheets are stacked in the simple +, − sequence. The repeat distance is the same as the chemical unit cell. The magnetic phase diagram, together with the temperature dependence of the magnetic moment, is shown in Fig. 9. The high-temperature region is schematic. The change from the 4+, 4− magnetic structure to the +, − arrangement has interesting consequences in the magnetization, low-temperature x-ray, and electrical-resistivity measurements. In Table II we present the neutron intensities of the $(111)^{-n}$ satellites as calculated for all possible square-wave models that involve eight layers. The values have been normalized to the (110) reflection of the type-I ordering (model 1). A similar table, together with a more detailed discussion, may be found in the study of the compound $UP_{0.75}S_{0.25}$ by Lander, Kuznietz, and Cox.[5] In NpAs, unravelling the magnetic structure between 145 and 170 °K is complicated by the variation with temperature of the neptunium magnetic moment. For this reason, the data in Table II are not on an absolute scale. The initial structure is model 7, the 4+, 4− arrangement. Intensities less than ~15 in Table II cannot be detected if the ordered moment is less than $1.5\mu_B/Np$; therefore the $(111)^{-3}$ satellite cannot be observed at 160 °K. However, an important experimental observation is that the intensity of $(111)^{-2}$ is less than or equal to 10 at all temperatures. This excludes models 3–6 as possibilities in the transition region. In Fig. 9, we indicate a "mixed" region, in which models 1 (type-I ordering) and 2, as well as the last vestiges of the 4+, 4− structure (model 7) probably coexist.

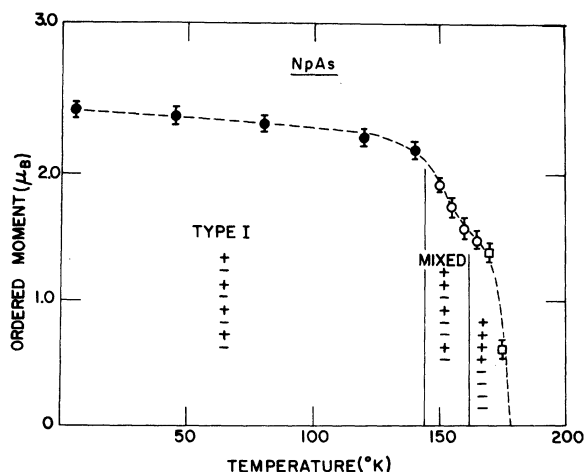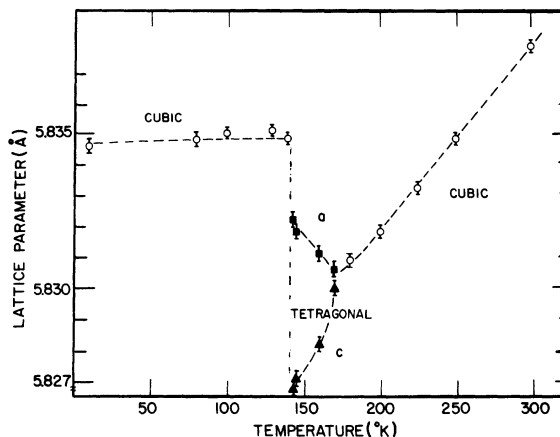The behavior of the lattice parameter of NpAs at low temperature (Fig. 10) has a number of strik-

FIG. 10. Variation of the lattice parameter of NpAs with temperature.

ing features. First, the material becomes tetragonal at 175 ± 2 °K, i.e., at T_N. Second, by 143 °K the c/a ratio has attained a value of 0.9992 ± 0.0002 and is varying in approximately the same manner as that of NpP (see Fig. 8). The value of c/a is derived from fitting a calculated profile, which includes the instrumental constants determined above the transition temperature, to the experimental points from the diffractometer output.[24] Third, on cooling to 142 °K, a first-order transition occurs such that the material becomes cubic again. A discontinuity in the volume of the unit cell is observed; the volume at 143 °K is 198.20 ± 0.07 Å³ and at 142 °K is 198.65 ± 0.05 Å³. Almost no hysteresis (≤ 0.5 °K) is associated with the 142 °K transition, and this is surprising in view of the large polycrystalline sample used in the experiments and the rather sluggish transition observed in the neutron experiments. One possibility is that the transition from tetragonal to cubic symmetry is essentially a cooperative one that occurs only when the total sample has transformed from the 4+, 4− to the +, − antiferromagnetic structure. Below 142 °K, the x-ray-diffraction peaks are broader than in the high-temperature cubic and tetragonal phases, possibly because of the influence of dynamic effects on the lattice parameter following the first-order transition. For example, the (444) reflection ($2\theta = 132°$) has a full width at half-maximum (FWHM) of $0.23° \pm 0.01°$ in the high-temperature cubic and tetragonal phases [the (444) reflection is not split by the tetragonal distortion], but has a FWHM of $0.27° \pm 0.01°$ at 140 °K. This width gradually decreases as the temperature is lowered, and the value at helium temperature is again $0.23°$. The absence of any tetragonal distortion at 5 °K may be characterized by the quantity $|(c-a)/a| \leq 3 \times 10^{-4}$.

The magnetization of NpAs as a function of tem-

FIG. 9. Magnetic phase diagram and the ordered magnetic moment per neptunium atom in NpAs as a function of temperature.
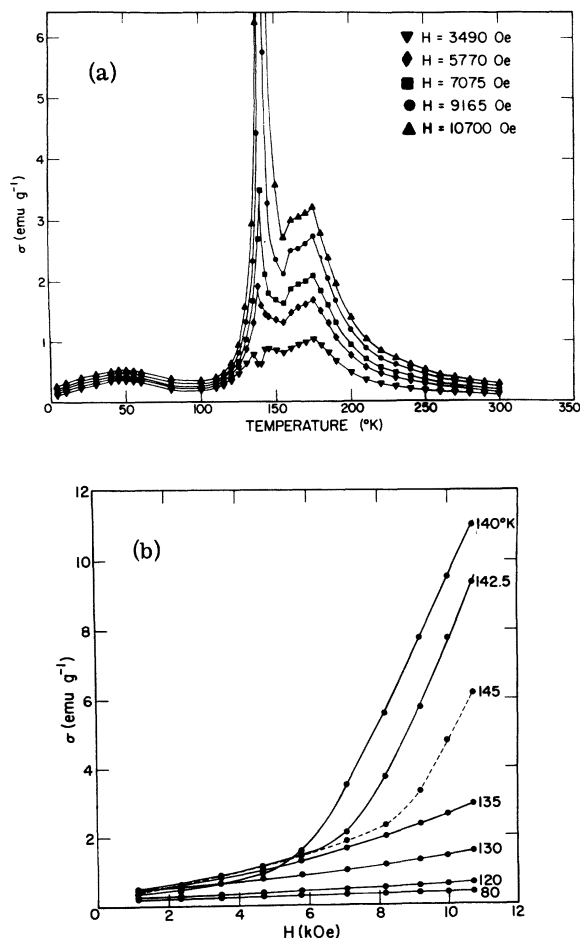
FIG. 11. (a) Magnetization of NpAs as a function of temperature for different applied magnetic fields. (b) Magnetization as a function of applied magnetic field for selected temperatures.

perature and field as shown in Fig. 11. The Néel temperature is indicated by a maximum in the magnetization at ~175 °K, but anomalous field-dependent behavior is observed between 150 and 140 °K. This is illustrated by plotting σ versus H for various temperatures in Fig. 11(b). The neutron experiments (see Fig. 9) indicate that the antiferromagnetic arrangement changes from the 4+, 4− scheme to the simple +, − ordering between 160 and 140 °K. Similar magnetization results were obtained by Crangle *et al.*[5] in $UP_{0.75}S_{0.25}$, in which the 5+, 4− structure changes to the type-IA structure (2+, 2−) at ~20 °K. A qualitative explanation for this unusual magnetic behavior in both NpAs and $UP_{0.75}S_{0.25}$ focuses attention on the coupling between adjacent ferromagnetic (001) planes in the antiferromagnetic structures. Near the transition temperature the coupling between these layers of magnetic moments changes, often from a ferromagnetic to an antiferromagnetic interaction (or

vice versa). Under these conditions, the stability of the antiferromagnetic structure may be destroyed and the sequence of layers rearranged by a magnetic field of several kOe. To test this hypothesis directly we plan to repeat the neutron experiments in an applied magnetic field.

The Mössbauer experiments on NpAs cannot give any information on the details of the magnetic behavior at ~140 °K, because, at this temperature, the recoil-free fraction is severely decreased. At 5 °K the hyperfine spectrum yields a single hyperfine field of 4800 ± 50 kOe. The spectrum at 5 °K is shown in Fig. 12 and should be compared with the more complicated spectrum observed for NpP at low temperature (Fig. 5) (The NpO_2 impurity in the Mössbauer spectrum is a consequence of the sample reacting with the lucite encapsulation material, and not a property of the original sample. For subsequent Mössbauer experiments on the other compounds the sample was encapsulated in an aluminum container.)

The electrical resistivity of NpAs is shown in Fig. 13. The magnitude of the resistivity at 300 °K is ~5100 $\mu\Omega$ cm. The antiferromagnetism is revealed as a small change in the slope of the resistivity curve at T_N. The most unusual feature of the data is that on cooling from 142 to 140 °K, the electrical resistivity increases by an order of magnitude. One possible explanation for this result is that NpAs changes from a semiconductor to a semimetal at the 142 °K transition. However, the resistivity does not have the exponential temperature dependence that would be expected if the material were a semiconductor below 142 °K. Another pos-
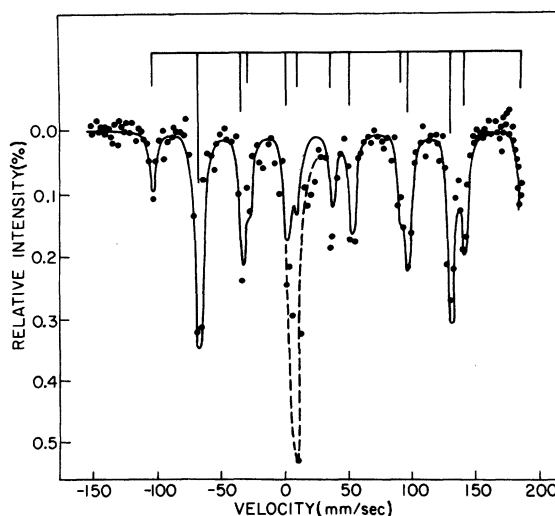

FIG. 12. Hyperfine spectra for ^{237}Np in NpAs at 5 °K. The solid curve is a least-squares fit to the data and yields the parameters of Table I. The dashed line is a spectrum from an NpO_2 contaminant (see text).
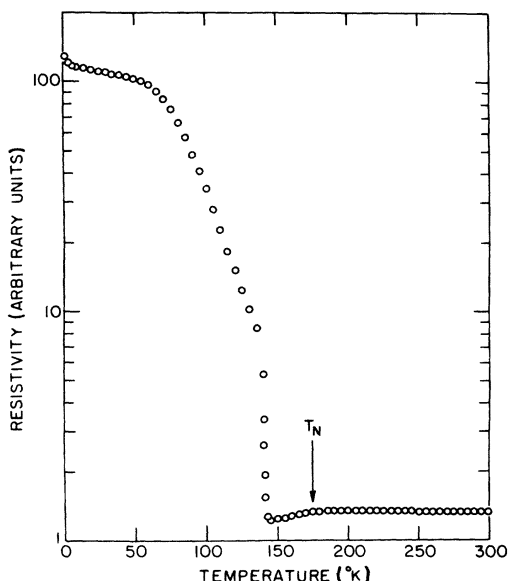
FIG. 13. Temperature dependence of the electrical resistivity of NpAs.

sible interpretation is that a valence change takes place in NpAs, but the other experimental measurements do not provide any supporting evidence for this interpretation. Finally, it might be argued that the first-order transition of the crystal structure at 142 °K causes a shift in the band structure and an abrupt change in the electrical properties of NpAs. This explanation also appears inadequate because the crystal structure below 142 °K is the same as the structure in the paramagnetic state above T_N, and the lattice parameters have comparable values in the two regions (see Fig. 10). Consequently, no dramatic changes in the conducting properties would be expected when the lattice transforms back to the cubic structure.

D. NpSb

The magnetic susceptibility[16] of NpSb as a function of temperature indicates an antiferromagnetic transition at 205 ± 2 °K. Below 175 °K the results are influenced by the presence of the impurity phase Np_3Sb_4 (see Sec. II), which becomes ferromagnetic at approximately this temperature. The magnetic structure of NpSb is type I at all temperatures below T_N. The temperature dependence of the square of the magnetic moment is shown in Fig. 14. At 5 °K the value of the ordered moment is (2.51 $\pm 0.07)\mu_B$/(Np atom). Also included in Fig. 14 is the $(J_{1/2})^2$ function normalized to $(2.51\mu_B)^2$ and $T_N = 207$ °K. Note the different behavior of NpN and NpSb relative to the $J_{1/2}$ function (Figs. 2 and 14).

The behavior of the lattice constant of NpSb as a function of temperature is quite normal, in that, as the temperature decreases, the rate of change of

the lattice constant with temperature also decreases. Thus, the lattice constants at helium temperature and 60 °K are almost identical. No anomaly is observed at the Néel temperature. The sample of NpSb was difficult to prepare. In addition to the extra phases, which do not, in general, affect the neutron, x-ray, or Mössbauer experiments, the homogeneity of the sample was poor. Accordingly, the reflections in the x-ray experiments were broad, as much as three times broader than the experimental resolution function measured on an annealed tungsten specimen at the same 2θ. Under these conditions, difficulty is encountered in defining the upper limit of a possible tetragonal (or rhombohedral) distortion, which, for small values of $(c-a)/a$, results in a broadening of the x-ray line profile. Consequently, a rather high value of $|(c-a)/a| \leq 15 \times 10^{-4}$ is given in Table I. However, any distortion that occurs at T_N would, in all probability, have a magnitude $> 20 \times 10^{-4}$ at helium temperature, and would therefore be readily observed in the low-temperature x-ray pattern.

The parameters determined from the Mössbauer experiment at 5 °K are given in Table I. No resistivity measurements were performed on NpSb because of the presence of additional phases.

IV. DISCUSSION

Any attempt to understand quantitatively the magnetic behavior of the neptunium monopnictides is clearly a complex task. Not only does this behavior vary from compound to compound in a complicated manner, but experiments on other actinide com-
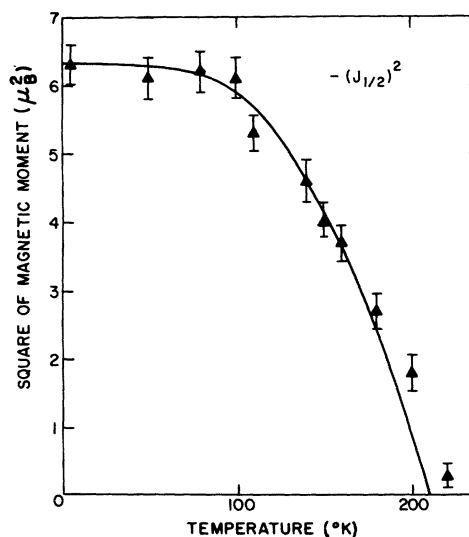

FIG. 14. Variation of the square of the ordered moment in NpSb with temperature. The ordering is type I at all temperatures. The solid line is the $(J_{1/2})^2$ function.
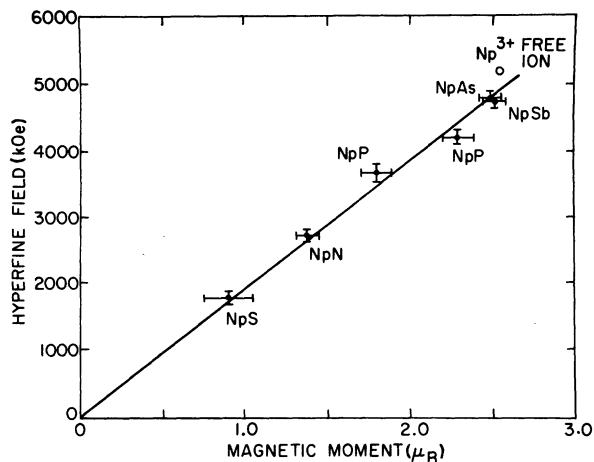
FIG. 15. Relationship between the magnetic hyperfine field H_{hf} (obtained by the Mössbauer effect) and the ordered magnetic moment (obtained by neutron diffraction) for the Np ion in NaCl-type compounds.

pounds (except those containing uranium) are sparse. As a start we pose three questions. (a) Is the magnetic behavior typical of localized or itinerant electrons? (b) How important is the presence of an orbital angular magnetic moment and the resultant electrostatic crystal field in determining the magnetic properties? (c) What is the mechanism of exchange in the magnetically ordered state? Of course, no simple answers can be given to such general questions, but the present experiments do aid in establishing trends that, in turn, may suggest the direction of further experiments and theory.

We interpret the results of the present experiments, as well as those on isostructural uranium compounds,[1] as evidence for localized $5f$ magnetic moments on the actinide ions. The ordered and effective magnetic moments for the free-ion Np^{3+}: $5f^4$ configuration, based on an intermediate-coupling g value, are $2.6\mu_B$ and $2.9\mu_B$, respectively.[25] The experimental values for the effective magnetic moments in the paramagnetic state are between $2.3\mu_B/$ (Np ion) and $2.8\mu_B/$(Np ion) (see Table I). The ordered moments are somewhat less than $2.6\mu_B$, which suggests the presence of crystal-field effects. In addition, the ratio of the ordered to the effective magnetic moment is between 0.6 and 0.9 for all compounds. These experimental values support a localized description of the magnetic moments.[26]

The quadrupole interactions measured in the Mössbauer experiments provide additional evidence concerning the configuration of the Np ions. In NpAs at 4.2 °K the value of e^2qQ is -70×10^{-7} eV. Since the cubic lattice is undistorted at this temperature, the electric field gradient arises only from oriented atomic electrons. Of the common Np

valencies (Np^{3+} to Np^{6+}), only Np^{3+} can give the observed negative interaction constant. Assuming a free-ion Hund's-rule $5f^4$ configuration, we calculate[27] $e^2qQ = -35 \times 10^{-7}$ eV, which compares reasonably well with experiment in view of the neglect of crystal-field effects and contributions from conduction-electron polarization.

In Fig. 15 the magnetic hyperfine fields obtained by the Mössbauer measurements are compared with the saturation magnetic moments as determined by neutron diffraction.[28] Also included is a point calculated[29] for free-ion Np^{3+} based on intermediate-coupling wave functions. The linear relationship shows that a unique, well-defined electronic configuration applies to all the compounds. The fact that the experimental points extrapolate to the Np^{3+} free-ion value argues both for the validity of this assignment and for the treatment of well-localized $5f$ electrons.

Since the wave functions of the $5f$ electrons are relatively more expanded than those of the $4f$ electrons, the crystal-field potential in the actinide series is even more important than in the lanthanide series. Unfortunately, the large spin-orbit and crystal-field interactions lead to the breakdown of the Russell–Saunders coupling scheme in the actinides. Lam and Chan[30] have recently shown that full J-mixing calculations must be performed to explain the magnetic properties of plutonium in ionic compounds. We anticipate that a similar situation exists for all actinide ions in metallic compounds. The number of f electrons must be determined before a crystal-field calculation can be attempted. This problem has been the source of much discussion in the Uv compounds,[31] and the answer is by no means obvious. Recently, in a study of UP, NpP, and PuP, Lam and Fradin[23] have analyzed the saturation moment and the temperature dependence of the paramagnetic susceptibility, the Knight shift, and the spin-lattice relaxation rate. They find that consistent results are found only with trivalent configurations, i.e., f^3 for UP, f^4 for NpP, and f^5 for PuP.

The role of the crystal field in determining the direction of the magnetic moments in the ordered state is difficult to establish. The crystal-field interaction within a single J manifold results in an easy direction for the magnetization that is readily calculated. Assuming that the fourth-order terms in the crystal-field potential are substantially larger than the sixth-order terms (as is the case in the lanthanide metallic compounds), the easy direction is $\langle 111 \rangle$ for $5f^1$, $5f^4$, and $5f^5$, and $\langle 100 \rangle$ for $5f^2$ and $5f^3$. On this basis, only NpN is consistent with a $5f^4$ configuration. Substantial evidence, however, suggests that such a simple scheme may not apply to the actinides. X-ray-diffraction experiments indicate that *all* ferromagnets examined so far [US,

USe, and UTe (all Ref. 19), NpN, and recent experiments in this laboratory on NpC] exhibit a rhombohedral distortion in the ordered phase. The easy axis of magnetization is therefore in, or perpendicular to, the (111) plane. On the other hand, with the possible exception of UO_2,[32] all actinide antiferromagnets examined by neutron diffraction have magnetic moments parallel to the cube edge. From these experimental facts, we conclude that the crystal field is not the dominating factor in determining the easy direction.

The Rudermann–Kittel–Kasuya–Yosida (RKKY) exchange, which arises from the s-f or d-f interactions, has been invoked to explain the nature of the exchange mechanism in actinide compounds.[1] Certainly, the long-range magnetic structure observed in the actinides for the first time in the UP-US solid solutions[5] suggests that the RKKY mechanism, which has been applied so successfully in the lanthanide series, can be used in the actinide series. Quantitative attempts to explain the ordering schemes, however, present a considerable challenge to theoreticians.[4] The incommensurate magnetic structures observed in the actinide compounds are not found in the lanthanide monopnictides, with the exception of CeSb.[33] These lanthanide compounds seldom order magnetically above 50 °K, suggesting that the exchange interactions are weaker than in the actinide monopnictides and monochalcogenides. A more apt comparison may therefore be made between the lanthanide metals and the actinide compounds. However, the lanthanide metals exhibit periodicities which vary with temperature, a consequence of the temperature dependence of the RKKY interaction and the topology of the Fermi surface,[34] and no such variations

with temperature in the periodicities of the magnetic structures have been observed in actinide compounds.[5] For example, in NpP the magnetic structure is incommensurate at T_N $(1/\tau = 2.78 \pm 0.08$ unit cells) and no variation of this periodicity is observed between 130 and 75 °K. At 74 °K an abrupt change to $1/\tau = 3.00 \pm 0.08$ unit cells occurs, and this commensurate periodicity remains unchanged on further cooling.

The magnetic transitions that occur in these compounds are closely coupled to the behavior of the lattice, as observed by x-ray diffraction. The volume change relative to the room-temperature value is shown in Fig. 16 as a function of temperature for each of the four compounds. At high temperatures the straight-line behavior reflects the regular thermal expansion of the lattice. The coefficients of thermal expansion are comparable to those of the uranium monopnictides. The volume contractions in NpN $(T_C = 87\ °K)$ and NpSb $(T_N = 207\ °K)$ vary smoothly through the transitions, indicating that they are not first order. Similarly, second-order transitions occur at T_N in NpP (125 °K) and NpAs (175 °K). However, at lower temperatures both NpP and NpAs exhibit first-order transitions, in which a discontinuity occurs in the volume of the unit cell.

In summarizing the magnetic properties of the neptunium monopnictides, it seems worthwhile to highlight some of the more unusual aspects. The nitride appears different from the other neptunium pnictides in that it has a lower ordered magnetic moment, is ferromagnetic, and has a ⟨111⟩, rather than a ⟨100⟩, easy axis of magnetization. (Uranium nitride also has an appreciably lower magnetic moment than the other Uv compounds.) Neptunium
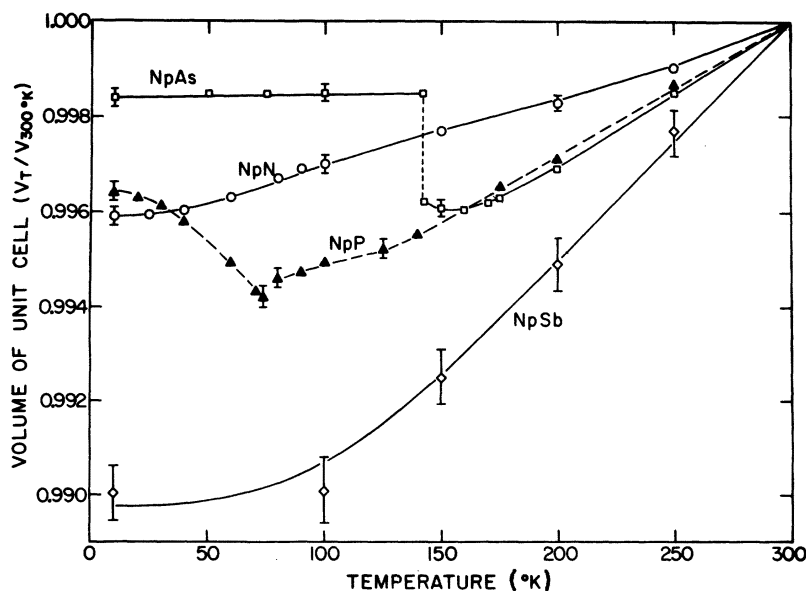

FIG. 16. Temperature dependence of the unit-cell volume (relative to the value at 300 °K) for the neptunium monopnictides.

phosphide has an incommensurate magnetic structure and, in addition, at the lowest temperatures the magnetic moments on all the metal atoms are not equivalent. A similar situation exists in $UAs_{0.68}S_{0.32}$.[6] A possible explanation for the variation of the magnetic moment from site to site in these magnetic structures is that an oscillatory magnetization contributed by the conduction electrons is superimposed on localized magnetic moments at the metal sites. In NpAs the transition from tetragonal to cubic symmetry (Fig. 10) *within the ordered regime* is, as far as we know, unique. Also associated with this remarkable lattice behavior is a large change in the electrical resistivity (Fig. 13). The general similarity of the magnetic structures of NpP and NpAs to that of $CeSb^{33}$ is particularly interesting. In cerium compounds, the *f* band lies close to the Fermi level, and the difficulties associated with understanding their magnetic properties are, in many respects, similar to those encountered in the actinide series.

In conclusion, the neptunium monopnictides present a plethora of fascinating magnetic behavior. We hope that the present report serves both as an illustration of the challenge of actinide magnetism and also as a spur to theoretical involvement in the subject.

ACKNOWLEDGMENTS

*Work performed under the auspices of the U. S. Atomic Energy Commission.

[1] For reviews of the properties of U*v* and U*vi* compounds, see J. Grunzweig-Genossar, M. Kuznietz, and F. Friedman, Phys. Rev. 173, 562 (1968); M. Kuznietz, in *Rare Earths and Actinides*, Conference Digest No. 3 (Institute of Physics, London, 1971), p. 162, and extensive references therein; F. A. Wedgwood and M. Kuznietz, J. Phys. C 5, 3012 (1972).

[2] For a review of the actinide metals, see M. B. Brodsky, AIP Conf. Proc. 5, 611 (1972).

[3] C. Long and Y. L. Wang, Phys. Rev. B 3, 1656 (1971).

[4] P. Erdos and J. M. Robinson, AIP Conf. Proc. 10, 1070 (1973); Phys. Rev. B 8, 4333 (1973).

[5] *Neutron diffraction*: M. Kuznietz, G. H. Lander, and Y. Baskin, J. Appl. Phys. 40, 1130 (1969); G. H. Lander, M. Kuznietz, and D. E. Cox, Phys. Rev. 188, 963 (1969). *X-ray diffraction*: M. Allbutt, R. M. Dell, A. R. Junkison, and J. A. Marples, J. Inorg. Nucl. Chem. 32, 2159 (1970); M. Kuznietz, F. P. Campos, and Y. Baskin, J. Appl. Phys. 40, 3621 (1969). *Magnetization*: M. Allbutt, R. M. Dell, A. R. Junkison, and J. A. Marples, J. Inorg. Nucl. Chem. 32, 2159 (1970); W. Trzebiatowski and T. Palewski, Phys. Status Solidi 34, K51 (1969); J. Crangle, M. Kuznietz, G. H. Lander, and Y. Baskin, J. Phys. C 2, 925 (1969). *Specific heat*: J. F. Counsell, R. M. Dell, A. R. Junkison, and J. F. Martin, Proc. Faraday Soc. (Lond.) 63, 72 (1967). *NMR*: M. Kuznietz, G. A. Matzkanin, and Y. Baskin, Phys. Rev. 187, 737 (1969); F. Friedman and J. Grunzweig-Genossar, Phys. Rev. B 4, 180 (1971).

[6] *Magnetization*: W. Trzebiatowski and T. Palewski, Bull. Acad. Polon. Sci. Ser. Sci. Chim. 19, 83 (1971). *Neutron diffraction*: J. Leciejewicz, A. Murasik, R. Troc, and T. Palewski, Phys. Status Solidi 46, 391 (1971); G. H. Lander, M. H. Mueller, and J. F. Reddy, Phys. Rev. B 6, 1880 (1972).

[7] *Neutron diffraction*: J. Leciejewicz, A. Murasik, T. Palewski, and R. Troc, Phys. Status Solidi 38, K89

(1970); 48, 445 (1971). *Magnetization*: T. Palewski, W. Suski, and T. Mydlarz, Int. J. Magn. 3, 269 (1972).

[8] R. J. Birgeneau, AIP Conf. Proc. 10, 1664 (1973); Y. L. Wang and B. R. Cooper, Phys. Rev. B 7, 2607 (1970), and references therein.

[9] A. W. Mitchell and D. J. Lam, J. Nucl. Mater. 39, 219 (1971).

[10] J. W. Ross and D. J. Lam, Phys. Rev. 165, 617 (1968).

[11] B. D. Dunlap, G. M. Kalvius, S. L. Ruby, M. B. Brodsky, and D. Cohen, Phys. Rev. 171, 316 (1968).

[12] Neutron Diffraction Commission, Acta Cryst. A 28, 357 (1972).

[13] G. H. Lander and T. O. Brun, J. Chem. Phys. 53, 1387 (1970).

[14] M. B. Brodsky, N. J. Griffin, and M. D. Odie, J. Appl. Phys. 40, 895 (1969).

[15] C. H. de Novion and R. Lorenzelli, J. Phys. Chem. Solids 29, 1901 (1968).

[16] D. J. Lam. AIP Conf. Proc. 5, 892 (1972).

[17] W. E. Gardner and T. F. Smith, in Proceedings of the Eleventh International Conference on Low Temperature Physics, St. Andrews, 1968, Vol. 2, p. 1377 (unpublished).

[18] F. A. Wedgwood, J. Phys. C 5, 2427 (1972).

[19] J. A. C. Marples, J. Phys. Chem. Solids 31, 2431 (1970).

[20] G. H. Lander, B. D. Dunlap, D. J. Lam, A. Harvey, I. Nowik, M. H. Mueller, and A. T. Aldred, AIP Conf. Proc. 10, 88 (1973).

[21] G. H. Lander, B. D. Dunlap, M. H. Mueller, I. Nowik, and J. F. Reddy, Int. J. Magn. 4, 99 (1973).

[22] M. H. Mueller, G. H. Lander, H. W. Knott, and J. F. Reddy, Phys. Lett. A 44, 249 (1973).

[23] D. J. Lam and F. Y. Fradin, Bull. Am. Phys. Soc. 18, 329 (1973); Phys. Rev. B 9, 238 (1974).

[24] M. H. Mueller, G. H. Lander, H. W. Knott, and J. F. Reddy, 19th Annual Conference on Magnetism and Magnetic Materials, Boston, 1973 AIP Conf. Proc. (to be published).

[25] D. J. Lam, B. D. Dunlap, A. T. Aldred, and I. Nowik, AIP Conf. Proc. 10, 83 (1973).

[26]S.-K. Chan, J. Phys. Chem. Solids 32, 1111 (1971).

[27]B. D. Dunlap, in *Mössbauer Effect Methodology*, edited by I. J. Gruverman (Plenum, New York, 1971), Vol. 7, p. 137. We have a Sternheimer factor $R_Q = 0.35$.

[28]For NpS see D. J. Lam, B. D. Dunlap, A. R. Harvey, M. H. Mueller, A. T. Aldred, I. Nowik, and G. H. Lander, International Conference on Magnetism, Moscow, 1973 (unpublished).

[29]The hyperfine-field calculation, including an estimate of core polarization, is discussed by B. D. Dunlap and G. M. Kalvius, Int. J. Magn. 2, 231 (1972).

[30]D. J. Lam and S.-K. Chan, Phys. Rev. B 6, 307 (1972).

[31]M. Allbutt and R. M. Dell, J. Inorg. Nucl. Chem. 30, 705 (1968); Z. Fisk and B. R. Coles, J. Phys. C 3, L 104 (1970); J. Grunzweig-Genossar, Solid State Commun. 8, 1673 (1970).

[32]B. C. Frazer, G. Shirane, D. E. Cox, and C. E. Olsen, Phys. Rev. 140, A1448 (1965).

[33]B. Lebech, P. Fischer, and B. D. Rainford, in *Rare Earths and Actinides* (Institute of Physics, London, 1971), p. 204.

[34]A. J. Freeman, in *Magnetic Properties of Rare-Earth Metals* (Plenum, New York, 1972), p. 245.